Proceedings of the 3rd Croatian Conference on Earthquake Engineering - 3CroCEE
19–22 March 2025, Split, Croatia

DOI: https://doi.org/10.5592/CO/3CroCEE.2025.28

SHAKE TABLE TESTING OF U-SHAPED MASONRY STRUCTURES: OUT-OF-PLANE RESPONSE TO VARYING GROUND MOTION SIGNALS

Babar Ilyas [(1)], Dario Vecchio [(2)], Nuno Mendes [(3)], Paulo B. Lourenco [(4)]

[(1)] *PhD Student, University of Minho, ISISE, Department of Civil Engineering, babarilyas7@gmail.com*
[(2)] *PhD Student, University of Minho, ISISE, Department of Civil Engineering, dariovecchio4@yahoo.it*
[(3)] *Auxiliar Researcher, University of Minho, ISISE, Department of Civil Engineering, nunomendes@civil.uminho.pt*
[(4)] *Full Professor, University of Minho, ISISE, Department of Civil Engineering, pbl@civil.uminho.pt*

Abstract

Historical structures consisting of unreinforced masonry are highly vulnerable to seismic forces, with out-of-plane failure mechanisms being a primary concern. This vulnerability has often resulted in the collapses of the masonry structures during seismic events. Masonry walls tend to rock and overturn in the out-of-plane direction due to the dynamic loading, leading to either one-way or two-way bending. These mechanisms mainly depend on the boundary conditions and the degree of connectivity between the structural elements. Previously the one-way and the two-way bending mechanisms of masonry structures have been explored to some extent. However, research is still needed to develop reliable analytical and numerical models for predicting the mechanism under seismic action. This paper presents an extensive experimental campaign carried out on the shake table at the University of Minho (PT) to assess the sensitivity of the out-of-plane behavior of U-shape structures to varying ground motions. Two signals were chosen from the database to enable a comprehensive analysis of how different types of seismic events influence the structural response. To replicate the behavior of historical unreinforced masonry structures, the specimen was constructed using dry-stack granite blocks in U-shaped configuration, consisting of a façade and two orthogonal walls. Dry joints allow the walls to be rebuilt after each test, ensuring the repeatability at large displacements. The structural response was evaluated under varying intensities of two distinct ground motion inputs. The outcomes of the experimental campaign are expected to contribute to the development of better predictive models for seismic risk assessment and conservation strategies for historical URM structures.

Keywords: Shake-table Testing, Out-of-Plane, Historical Structures, Unreinforced Masonry, Collapse Mechanism.

1. Introduction

Unreinforced masonry (URM) structures make up a substantial portion of the architectural heritage in many earthquake-prone regions, such as Italy, Portugal, and Greece, where they also reflect profound cultural and historical significance [1]. These structures are typically built with thick vertical load-bearing walls without consideration for lateral seismic actions, making them highly vulnerable to earthquake-induced damage. This observation is supported by many post-earthquake in-situ observations. For example, the February 6, 2023, Kahramanmaras Earthquake occurred in Turkiye, demonstrating the destructive effects of seismic activity on masonry structures, further emphasizing the importance of addressing their vulnerability [2]. In New Zealand, for instance, URM built heritage is a vital element of the architectural landscape, yet, it represents a severe vulnerability under seismic activity [3]. Similarly, in India, the wide prevalence of URM buildings in densely populated urban areas under high seismic vulnerability highlights the potential for catastrophic outcomes during earthquakes [4]. Therefore, it is apparent the urgent need to protect such structures, to avoid human casualties and economic losses. Research has consistently shown that URM structures frequently sustain damage and experience collapses when subjected to seismic forces because of their limited tensile strength, brittle nature, and lack of lateral resistance [5]. This vulnerability to cracking, severe damage, and collapse

DOI: https://doi.org/10.5592/CO/3CroCEE.2025.28

under seismic loads is often increased by non-ductile construction techniques such as the absence of reinforcement and the rigid connections between structural components [6]. However, a complete understanding of all the possible mechanisms of energy dissipation, the occurrence of large displacements and the probability of collapses is still not completely understood, especially when dealing with dynamic forces.

Depending on their direction, URM walls can experience both in-plane (IP) and out-of-plane (OOP) collapse mechanisms during an earthquake event. Largely and yet not clearly understood are the OOP mechanisms that have proven to be highly destructive due to the tendency of masonry walls to rock and overturn, leading to sudden collapses and substantial damage [7]. They are triggered in situations of poor connection between the façade and diaphragm/roof systems, when the seismic forces act perpendicular to the walls. They can result in pronounced rocking, bending, and eventually overturning, as illustrated in **Figure 1.** The OOP vulnerability has been observed in numerous earthquake events, where URM have exhibited distinctive one-way and two-way bending mechanisms influenced by various factors such as boundary conditions, degree of connectivity between structural elements, and slenderness ratios.

Figure 1. OOP failure mechanisms observed in URM structures [8].

One-way bending mechanisms are due to either poor lateral connection between two elements or the presence of an opening. Upon the existence of such a configuration, a wall/panel may undergo a sustained rocking motion over the base, after the creation of a three-hinge system. Two hinges are formed at the top and the bottom boundary conditions, while the latter forms along the height of the wall/panel [9]. This failure was also observed in isolated walls which have insufficient later support along the vertical edges. As a result, they exhibit significant rotational displacement, which leads to the complete overturning of the wall, especially when the slenderness ratio is high [10]. In contrast, two-way bending mechanisms involve both horizontal and vertical bending, creating more complex displacement patterns and rotational behavior. The two-way mechanism has been observed in wider facades, supported by structural elements or boundary conditions that prevent free OOP displacements, but allow rotations on both vertical and horizontal edges [7].

DOI: https://doi.org/10.5592/CO/3CroCEE.2025.28

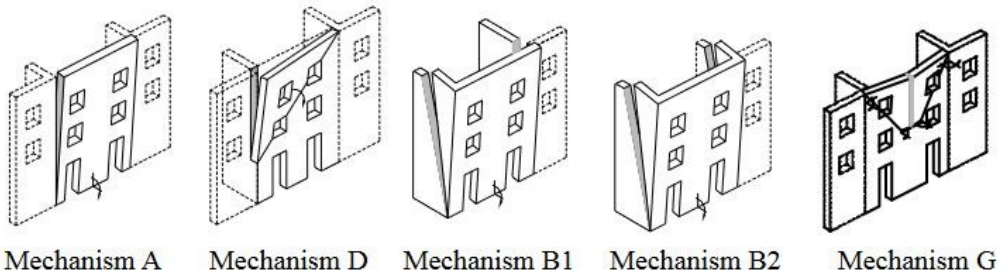

Figure 2: Example OOP mechanisms reported in various studies [11].

As shown in **Figure 2,** many OOP mechanisms in URM structures have been previously investigated with the use of analytical and numerical models. However, most of these studies focused on a priori selection of a specific mechanism and the application of quasi-static loading patterns. Despite the highly non-linear problem, force and displacement-based static tools lack the accuracy needed to predict the seismic response/capacity of URM under dynamic loading. In addition, due to the complex interaction between the characteristics of a ground motion, these models often lead to overly conservative strengthening and retrofitting solutions [12].

As mentioned, several factors, such as walls' geometry, boundary conditions, degree of connectivity between structural elements, and type of seismic excitation, may contribute to the complex nature of OOP collapse mechanism. This highlights the necessity of developing reliable analytical and numerical models to predict the capacity of OOP mechanisms, based on the dynamic response of URM structures. Such analytical and numerical models are crucial for assessing structural safety and guiding retrofitting efforts, particularly in historical contexts where structural interventions must be minimized to conserve heritage value. However, the accuracy of these models depends on the calibration and validation against extensive experimental data. Indeed, the existing studies have primarily focused on more straightforward configurations or limited testing scenarios, leaving a gap in comprehensive OOP assessment for more varying scenarios in terms of seismic excitations.

Shake table testing is one of the most advanced techniques used for experimental dynamic testing, because it can replicate real ground excitations in a controlled laboratory environment. Numerous studies have used shake table testing to assess the behavior of both reinforced and URM under varying seismic intensities and geometric configurations [7], [13], [14], [15], [16]. However, previous studies have largely concentrated on simpler wall configurations, often overlooking the distinctive structural behavior of 3D masonry systems under seismic forces. Additionally, the effect of varying ground motion signals on OOP responses remains insufficiently investigated. This paper addresses this gap by conducting an extensive experimental campaign within the framework of the Stand4Heritage project. The Stand4Heritage project aims to develop new standards and methodologies for seismic assessment and preservation of built cultural heritage. Dry-stacked granite blocks configured in a U-shape assembly, consisting of a façade and two orthogonal walls, are tested on the shake table at the Structural Laboratory of the University of Minho (PT). Through the application of two different ground motion signals on the same specimen, this study provides a broader understanding of how URM structures behave in the OOP direction under excitations of different characteristics. In the following sections the experimental campaign is presented including the test setup, ground motion signals selection and the outcomes of the campaign.

2. Experimental Setup

2.1. Description of Specimen

The experimental study used a U-shape URM specimen, constructed with dry-joint masonry blocks to replicate the seismic vulnerability of historical masonry structures. The specimen's configuration consisted of a 1.5-meter-long façade wall oriented perpendicular to the direction of the shake table's

DOI: https://doi.org/10.5592/CO/3CroCEE.2025.28

motion to allow the occurrence of OOP failure mechanisms. Each return wall measured 1.65 m in length, connected to the facade forming a U-shape configuration.

The specimen has a total height of 1.5 m, constant across all the walls. Two types of blocks were used, and they are as follows: (a) Type 1, with dimensions of 30 cm x 30 cm x 15 cm, (b) Type 2 with dimensions of 15 cm x 15 cm x 15 cm. The masonry was built with granite blocks, disposed of in a typical stretcher bond pattern. The use of dry-stacked granite blocks, typical of historical masonry practices (especially in the country of Portugal), allowed for easy disassembly and reassembly, enhancing the repeatability in successive tests under varied seismic inputs. **Figure 3(a)** shows a view of the specimen constructed on the top of the shake table.

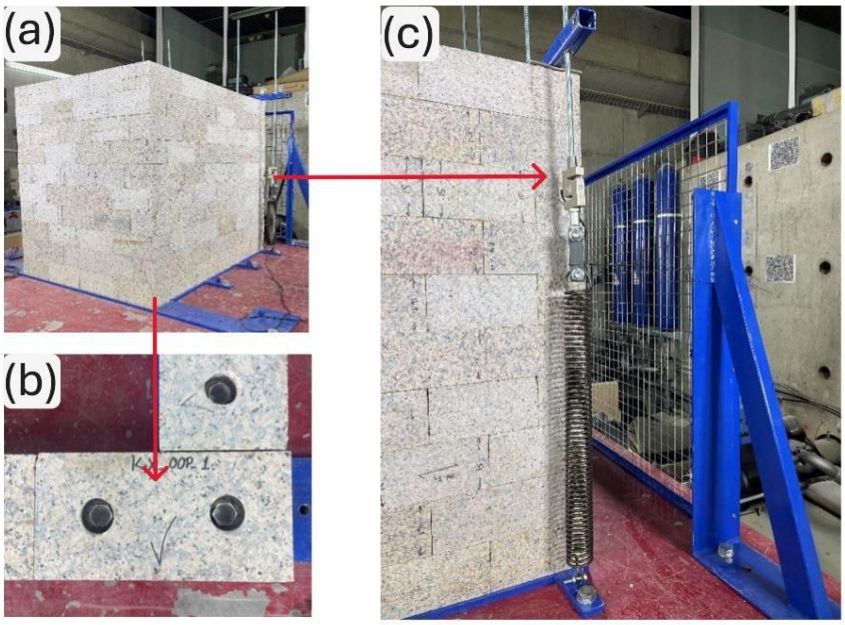

Figure 3: Test setup: (a) U-shape specimen, (b) anchoring system of the base course, and (c) spring-load cell connection in the precompression system.

2.2.Shake Table Specifications

The shake table facility available at the Structural Laboratory at the University of Minho, (PT) was used for this extensive experimental campaign. The shake table has a platform of 2.9 m x 2.9 m, with one degree of freedom (DOF), i.e., unidirectional. The shake table is operated by a hydrodynamic actuator, working up to a pressure of 300 kN, thus allowing the construction of specimens up to 3 tons. Note that the shake table weighs 3 tons. The shake table can work within a frequency range of 0-50 Hz, which covers the typical relevant frequency range for civil engineering structures. The main features of the shake table are given in **Table 1**. The shake table is equipped with a control station comprising two chassis. The primary chassis manages system operations, including the actuator's hydraulic system, while the secondary chassis offers expansion capabilities for additional instrumentation as needed. The surface of the shake table is provided with a grid of M27 holes, enabling bolted connections to anchor specimens directly to the platform, which is critical for simulating realistic seismic conditions without slippage or unintended movement. **Figure 4** shows a view of both the shake table and actuator.

Table 1: Shake table features.

Dimensions [m]	Frequency [Hz]	PTA[a] [g]	PTV[b] [cm/s]	PTD[c] [cm]	M_{ST}[d] [kg]	M_{ST}[e] [kg]
2.9 x 2.9	0-50	5	85	±12.5	3000	3000

a) Peak table acceleration, b) Peak table velocity, c) Peak table displacement, d) Mass of shake table, e) Maximum payload

DOI: https://doi.org/10.5592/CO/3CroCEE.2025.28

Figure 4: The 1DOF shaking table installed at the University of Minho (PT).

2.3. Test setup and Instrumentation

The specimen was designed with a height of 1.5 m, with a total of 10 horizontal courses. To replicate realistic boundary conditions, the base of the specimen was anchored to the shake table platform. Each masonry block in the first course was connected to steel plates using two M18 threaded bolts embedded within the blocks. Next, the plates were fixed to the shake table's platform with M27 bolts, thereby simulating a rigid foundation and preventing any unintended sliding during seismic excitation, as shown in **Figure 3(b)**.

At the ends of the east and west return walls, a precompression force of 2 kN was applied on each wall via spring mechanisms to further establish a fixed boundary condition, as shown in **Figure 3(c)**. No additional restraints were applied to the top of the façade, allowing for a free upper boundary. This configuration reflects the case of a façade poorly connected to either a diaphragm or a roof system, which has the potential of triggering a complete overturning (see **Figure 2**).

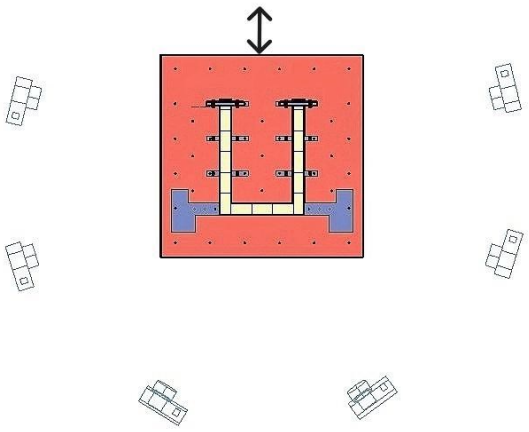

Figure 5: Schematic diagram of DIC cameras setup (top view).

To accurately capture the dynamic response of the masonry structure during testing, a Digital Image Correlation (DIC) system was employed as the data recording tool. The DIC system provides a contactless method of measurement, capable of recording displacement and strain data across the specimen surfaces. The system includes six high-speed cameras, each operating at a frequency of 145 Hz, ensuring that displacements are captured with high accuracy. The cameras were properly positioned surrounding the structure, with two cameras assigned to monitor each wall. **Figure 5** shows a top view of the camera location around the shake table (in red). This arrangement allowed for comprehensive, multi-angle coverage of the façade and both return walls, facilitating accurate data recording across the entire structure. Before testing, the cameras were calibrated and adjusted to account for lighting

Proceedings of the 3rd Croatian Conference on Earthquake Engineering - 3CroCEE
19–22 March 2025, Split, Croatia

DOI: https://doi.org/10.5592/CO/3CroCEE.2025.28

conditions. Also, the cameras were paired to create stereo vision, enhancing the system's ability to capture displacement and deformation accurately across the three-dimensional geometry of the specimen. Additionally, the table is featured by a high precision accelerometer (±5g), enabling the real-time monitoring of the peak table acceleration (PTA).

2.4. Testing Protocols

Considering the operational limits of the shake table, both selected ground motion signals required scaling to achieve the desired test intensities. The HOR signal, which exhibited moderately impulsive characteristics, was scaled up to twice its original amplitude, with increments of 25% applied for each test stage. Due to its less impulsive nature, the ARG2 signal was scaled to 3.5 times its original amplitude, maintaining the same 25% incremental increases. Before testing, according to well-known protocols, each scaled signal was calibrated to ensure response spectra matching by using equivalent rigid masses bolted on the shake table.

A low-amplitude pink noise signal having a frequency range of 0-50 Hz was used to conduct dynamic identification tests on the specimen. Dynamic identification tests aimed to determine the natural frequencies and their corresponding mode shapes to understand the dynamic characteristics of test the specimen.

The testing followed an incremental dynamic loading approach, divided into two phases: **General Run** and **Collapse Area**. In the General Run, the specimen was subjected to incremental increases, starting from a 0.25 scale factor up to 2.0 times the original PGA of HOR and up to 3.5 times for ARG2, with each increment of 25%. This phase provided a broad view of the structural response across a varying excitation level, with a major focus on the measured maximum displacement. In the second phase, tests were concentrated around specific PGAs, where collapses were observed. This stage aimed to deepen the understanding of the randomness of collapse occurrence, allowing the reconstruction of fragility curves.

3. Ground Motion Signal

Testing URM structures under a variety of ground motion signals is critical due to the unique responses caused by different seismic characteristics. Also, OOP mechanisms may be extremely sensitive to velocity rather than acceleration content. As a result, several numerical analyses have already focused on the URM response under pulse-like ground motions, which usually release most of the energy in small-period velocity pulses. By experimentally applying both impulsive and non-impulsive signals, researchers can replicate a broader spectrum of real-world seismic events, allowing a more comprehensive understanding of OOP failure mechanisms. This approach helps ensure that the structural responses observed during the tests closely reflect real-world conditions. Such a consideration is fundamental for URM structures, which are highly sensitive to changes in frequency, due to their non-linear behavior.

3.1. Selection and Characteristics of Ground Motion Signals

The selection of appropriate ground motion signals to investigate the OOP responses of URM structures was a critical aspect of this experimental campaign. Given the demanding nature of shake table testing, the selection of the signal was guided by two criteria: (1) each signal should be capable to initiate the targeted failure mechanisms, and (2) each signal had to comply with the operational limitations of the shake table, including capacity constraints in acceleration, velocity and displacement. The compliance with these criteria ensured that the selected signals would generate the desired seismic responses without exceeding the mechanical limits of the experimental setup.

The European Strong-Motion (ESM) database was used to search for potential candidate signals. Preliminary Non-Linear-Time-History-Analyses (NLTHA) based on a discontinuous model and the use of an explicit algorithm to facilitate the computational efforts, were conducted on 20+ ground motion records. According to the occurrence of collapses encountered in the NLTHAs, seven ground motion

DOI: https://doi.org/10.5592/CO/3CroCEE.2025.28

signals, as shown in **Table 2**, were shortlisted based on their capacity to induce significant rocking, overturning, and bending behavior.

Table 2: Ground motion suite selected for the dynamic campaign: main characteristics.

Event name	Year	M_w	PGA [g]	PGV [cm/s]	PGD [cm]	LDV*	IPR**	IP***
GMN	1976	6.4	0.33	37.26	4.12	337.56	1.0	9.06
NRC	2016	6.0	0.72	56.78	5.67	752.64	1.0	13.26
HOR	1998	6.2	0.37	35.16	3.82	532.93	1.0	15.16
NRC	2016	6.0	0.36	30.33	5.43	680.1	0.86	22.42
MZ28	2016	6.6	0.76	29.49	7.0	886.28	0.36	30.05
4629	2023	7.7	0.34	28.32	9.17	1090.9	0.04	38.52
ARG2	2014	6.2	0.35	21.65	3.49	861.56	0.02	39.8

* Development length of velocity time series, ** Impulsivity index by regression, *** Impulsivity index

3.2. Rationale for Categorizing Ground Motion Signals

Given the goal of investigating the pulse-like behavior on the U-Shape specimen, the seven ground motions were analyzed in terms of their impulsivity content. Such an analysis is based on the observation of the velocity time series to classify the pulse-like (impulsive) and non-impulsive signals [17]. The classification procedure involved the following steps:

1. **Development Length of Velocity (Ldv)**: The Ldv parameter was calculated for each ground motion signal by summing the incremental variation in velocity over time. The "length" of the velocity time history provides a quantitative measure of the impulsive nature of the signal, with shorter lengths typically associated with stronger impulsive characteristics. LDv was calculated using Eq. (1).

$$\mathrm{LDv} = \sum_{i+1}^{n} \left(\sqrt{(\Delta t)^2 + (\Delta V)^2}\right) \tag{1}$$

2. **Peak Ground Velocity (PGV)**: PGV was measured for each signal, representing the peak recorded value of velocity within its time history. This value, in combination with Ldv, helps to identify signals that exhibit sharp, high-velocity pulses indicative of impulsive signals.

3. **Impulsivity Index by Regression (IP_R):** A logistic regression model was used to predict the nature of a ground motion signal. This regression used PGV and Ldv values as predictors, assigning each signal to an impulsive category (e.g., impulsive or non-impulsive) based on historical earthquake records with known impulsive characteristics. This additional step minimizes subjectivity in impulsivity classification and provides a statistically backed approach to selecting signals. The IP_R was calculated using Eq. (2).

$$\mathrm{IP_R} = \frac{1}{1 + e^{(5 - 0.45(\mathrm{PGV}) + 0.01(\mathrm{LDv})}} \tag{2}$$

4. **Impulsivity Index (IP)**: IP is the ratio of development length of velocity time series to peak ground velocity. Lower IP values correspond to higher impulsivity, which is typical of pulse-like ground motions.

5.

6. **Table** *3* shows the thresholds to classify signals into different levels of impulsivity, allowing for the differentiation of highly impulsive signals from those with more distributed or vibratory characteristics [17]. The IP was calculated using Eq. (3):

$$\mathrm{IP} = \frac{\mathrm{LDv}}{\mathrm{PGV}} \tag{3}$$

DOI: https://doi.org/10.5592/CO/3CroCEE.2025.28

Table 3: Classification of Impulsivity Levels.

IP	Impulsivity
IP ≤ 12	Highly Impulsive
12 < IP ≤ 20	Moderate Impulsive
20 < IP ≤ 35	Low Impulsive

Using this classification, two signals were selected to provide the targeted OOP responses: one moderately impulsive signal and one less impulsive or vibratory signal. The first signal, recorded during the Azores Earthquake in 1998 (HOR), exhibited characteristics of a moderately impulsive event, making it suitable for testing immediate and forceful OOP responses. The second signal, from the 2014 Western Greece (ARG2) earthquake, represented a non-impulsive event. **Figure 6** shows the acceleration, the velocity, and the displacement time histories for each signal. By combining the results of the NLTHAs and regression-based impulsivity classification, this selection of two contrasting signals, one moderately impulsive and one non-impulsive, which supports the assessment of URM structures under variable seismic conditions.

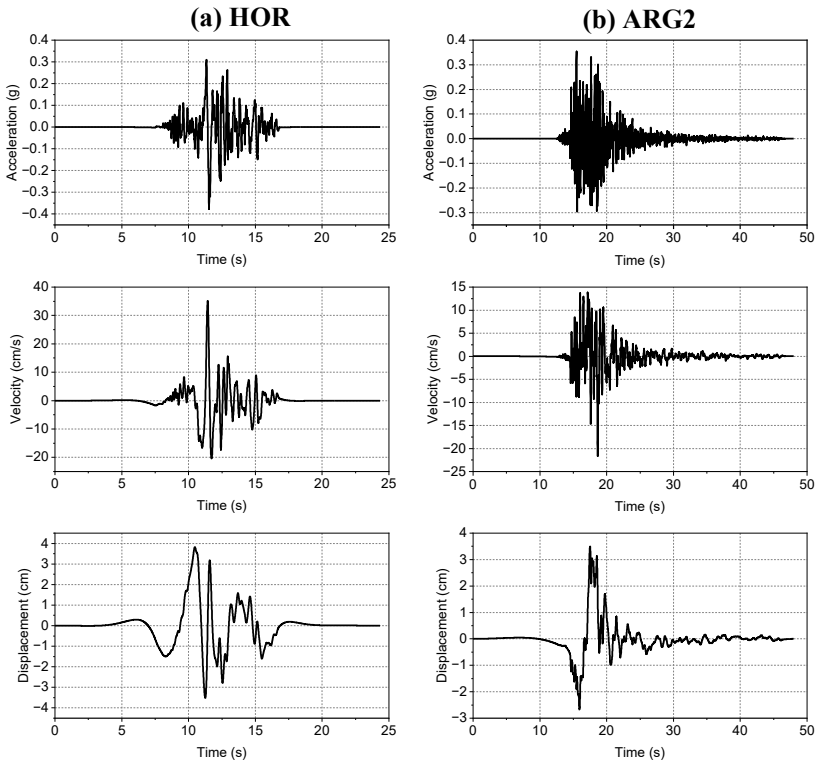

Figure 6: Time histories of the signals: (a) HOR, (b) ARG2.

4. Observed Structural Response

The U-shape specimen was subjected to incremental dynamic testing using the two ground motion signals, namely HOR and ARG2, selected using the criteria mentioned above. For each test, the specimen was returned to its original undamaged state, allowing for the assessment of distinct failure mechanisms at varying intensity levels.

DOI: https://doi.org/10.5592/CO/3CroCEE.2025.28

4.1.Impulsive Signal

The response of the specimen under the moderate impulsive ground motion was a complex occurrence of two distinct mechanisms, the horizontal bending of the façade, due to the return walls' opening, and the overturning of the façade, due to shear-diagonal cracking in the orthogonal walls. Note that in the case of dry-stacked masonry structures, cracking is associated with detachment of the blocks at the common interface. At low PGA levels, up to 0.2g, the structure remained stable with no notable damage. Minor bending of the façade was first observed around 0.25g, though without any substantial cracking or structural damage. This response suggested that the specimen could initially withstand low-to-moderate seismic forces without substantial impact. As the PGA increased beyond 0.3g, more visible deformation was observed in the top courses of the façade, however, the overall response was still dictated by the bending of the façade. Around 0.4g, the response started showing a combination of bending and (minor) rocking, suggesting the initiation of a complex dynamic OOP response, where the shift from one to the other mechanism was dictated by the increasing energy of the velocity pulse. Around 0.5g, the structure exhibited higher interaction between bending forces and rocking, particularly in the façade and at the connections with the return walls, where diagonal cracks were highly visible.

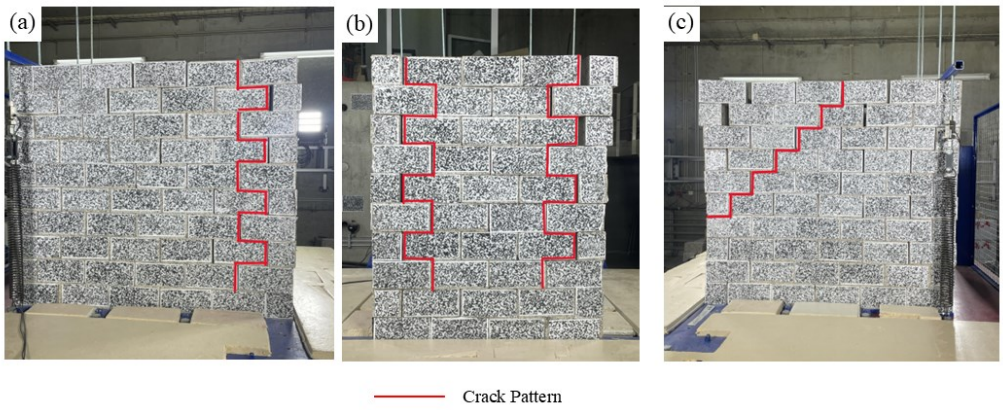

Figure 7: Observed damage before the collapse at 0.524 g: (a) interface separation of the facade from west return wall, (b) return walls opening seen in the facade, and(c) diagonal crack in the east return wall.

In the higher intensity range, specifically between 0.5g and 0.6g, the deformation pattern became significantly more pronounced. Large residual displacements were evident in the façade, and the cracks at the junctions between the façade and return walls widened. At 0.56g, substantial deformation was observed in the façade, accompanied by noticeable separation at the interface with the return walls. This stage marked a critical threshold for structural stability, as further increases in PTA pushed it towards collapse. **Figure 7** illustrates the residual deformation in the façade and the cracking patterns in the return walls. At a PTA of around 0.6g, the façade underwent a partial collapse due to overturning, with recorded peak table velocity (PTV) and peak table displacement (PTD) values of 54.41 cm/s and 5.61 cm, respectively.

DOI: https://doi.org/10.5592/CO/3CroCEE.2025.28

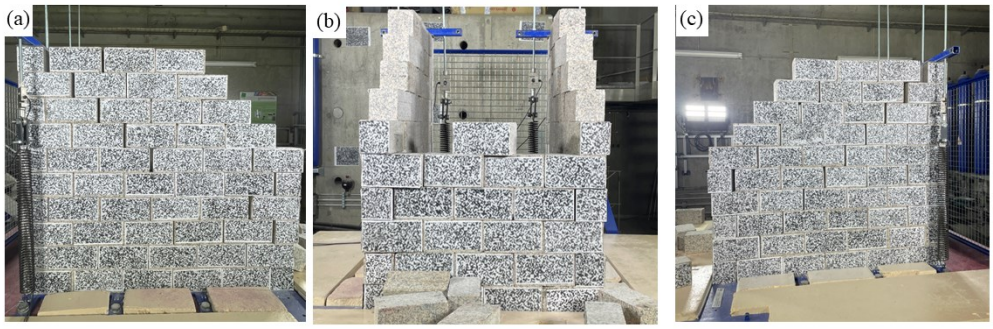

Figure 8: Observed collapse at 0.766 g: (a) top corner of the west return wall involved in the collapse, (b) overturning of the façade, and (c) widened diagonal cracks in the east return wall.

The collapse was characterized by concentrated damage in the OOP façade, where blocks in the upper courses began to separate and dislodge. Concurrently, significant diagonal cracking extended from the base to the top corners of the return walls, reflecting intense lateral stresses acting on these elements. Although the overall testing showed the development of symmetric deformation patterns, notable variations were noted between the left and right sides of the structure. This clearly suggested the existence of asymmetric in the structure, despite the application of a 1 DOF signal input.

At PGAs exceeding 0.7g, the façade experienced all collapse, with widespread block separation and substantial dislodgement along the upper courses. The return walls, although exhibiting extensive diagonal cracking, resisted full overturning due to their in-plane stiffness, which provided some degree of lateral stability despite severe damage. **Figure 8** captures the post-collapse condition of the façade, along with the diagonal cracks that formed in the return walls.

4.2.Non-Impulsive Signal

The structural response of the U-shape URM specimen to the non-impulsive ARG2 ground motion signal differed notably from the behavior experienced under the impulsive HOR signal. At lower PTAs (up to approximately 0.5g), the specimen displayed mild rocking and bending, characterized by incremental lateral displacements in both the façade and return walls. These early displacements were not accompanied by significant structural damage, suggesting that the initial phases of this non-impulsive signal allowed the structure to accommodate seismic forces with minimal deformations. As the PTA increased beyond 0.5g, bending became visible in the upper courses of the façade, along with the formation of diagonal cracks in the return walls. These cracks gradually widened with increased loading but did not immediately compromise structural stability, indicating a tolerance for progressive deformation under non-impulsive forces. At higher PTAs, nearing 1.0g, the specimen continued to display OOP bending and rocking without the sudden collapse observed. Prominent OOP bending mechanism was observed in the façade which extended down to the lower courses, as illustrated in **Figure 9**. Residual displacement in the return walls was higher because of the very high intensity of this vibratory signal. The collapse was first observed at a PTA of 1.31g, where the recorded PTV and PTD were 63.4 cm/s and 11.93 cm, respectively.

DOI: https://doi.org/10.5592/CO/3CroCEE.2025.28

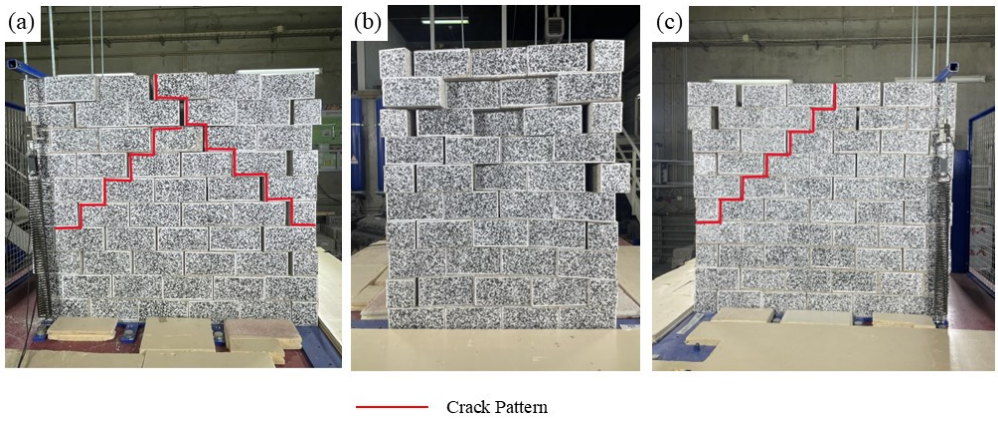

Figure 9: Observed damage before collapse at 1.14 g: (a) crack opening due to in-plane rocking of two macro-blocks in west return wall, (b) displaced blocks in OOP façade shows bending and opening of return walls, and (c) large displacements in east return wall along with crack showing formation of macro-blocks.

The failure mechanism, in this case, was markedly different from that under impulsive loading; the collapse occurred gradually, initiated by progressive rocking and severe bending in the façade along with the outward opening of the return walls. In-plane rocking was also observed in both return walls, forming two macro-blocks in the return walls. This behavior led to a gradual dislodgement of blocks, particularly in the upper courses of the façade, rather than a sudden collapse. **Figure 10** captures the state of the structure following the initial collapse, showing both the gradual dislodgement of the facade, and the damage progression in the return walls.

Figure 10: Observed collapse at 1.31 g: (a) top corner involved in collapse along with a wide diagonal crack in the west return wall, (b) Disintegration of the blocks in the facade, and (c) separation of interfaces with wide cracks in the east return wall.

5. Conclusion

This paper describes a shake table campaign conducted on a U-Shape dry-stacked masonry specimen to enhance the understanding of the out-of-plane collapse mechanism of unreinforced masonry structures under varying seismic ground motion characteristics. By applying both impulsive and non-impulsive ground motion signals, the experiments revealed distinct structural responses to each type. The impulsive signal triggered rapid damage progression and sudden collapse due to overturning in the façade, with significant diagonal cracking in the return walls. In contrast, the non-impulsive signal allowed for a gradual rocking and bending response, delaying collapse initiation even at higher peak ground accelerations. Thus, the final collapse was dictated by the higher frequency content in the acceleration time history, rather than by a significant pulse in the velocity time history. It was possible to state that the collapse happened due to the disintegration of the masonry.

DOI: https://doi.org/10.5592/CO/3CroCEE.2025.28

Notably, the impulsive HOR signal led to collapse at lower PTA, PTV, and PTD levels than the non-impulsive ARG2 signal, underscoring the significant influence of ground motion impulsivity on URM structural failure mechanisms. These findings highlight the importance of incorporating ground motion characteristics into seismic assessments, especially for historical masonry structures.

Finally, this research underscores the need for predictive models that account for ground motion impulsivity when evaluating URM seismic vulnerability. The results emphasize the value of using varied seismic signals in experimental testing to capture realistic structural responses, contributing to the creation of valuable data for the conservation of heritage masonry structures in earthquake-prone areas.

Acknowledgements

This investigation has been partly funded by the STAND4HERITAGE project that has received funding from the European Research Council (ERC) under the European Union's Horizon 2020 research and innovation program (Grant agreement No. 833123), as an Advanced Grant. This work was also partly financed by FCT/MCTES through national funds (PIDDAC) under the R&D Unit Institute for Sustainability and Innovation in Structural Engineering (ISISE), under reference UIDB/04029/2020, and under the Associate Laboratory Advanced Production and Intelligent Systems ARISE under reference LA/P/0112/2020.

References

[1] C. Modena, F. Da Porto, and M. Valluzzi, Eds., Brick and Block Masonry: Proceedings of the 16th International Brick and Block Masonry Conference, Padova, Italy, 26-30 June 2016. CRC Press, 2016. doi: 10.1201/b21889.

[2] V. Kahya et al., "Evaluation of earthquake-related damages on masonry structures due to the 6 February 2023 Kahramanmaraş-Türkiye earthquakes: A case study for Hatay Governorship Building," Eng. Fail. Anal., vol. 156, p. 107855, Feb. 2024, doi: 10.1016/j.engfailanal.2023.107855.

[3] A. Marotta, L. Sorrentino, D. Liberatore, and J. M. Ingham, "Seismic Risk Assessment of New Zealand Unreinforced Masonry Churches using Statistical Procedures," Int. J. Archit. Herit., vol. 12, no. 3, pp. 448–464, Apr. 2018, doi: 10.1080/15583058.2017.1323242.

[4] R. Maheshwari, B. K. Singh, and R. Marques, "Seismic vulnerability assessment and strengthening of an existing typical Indian unreinforced masonry building in a high-risk seismic zone-a comprehensive application," Innov. Infrastruct. Solut., vol. 9, no. 11, p. 424, Nov. 2024, doi: 10.1007/s41062-024-01728-7.

[5] D. D'Ayala and E. Speranza, "Definition of Collapse Mechanisms and Seismic Vulnerability of Historic Masonry Buildings," Earthq. Spectra, vol. 19, no. 3, pp. 479–509, Aug. 2003, doi: 10.1193/1.1599896.

[6] S. Cattari, M. Angiolilli, S. Alfano, A. Brunelli, and F. De Silva, "Investigating the combined role of the structural vulnerability and site effects on the seismic response of a URM school hit by the Central Italy 2016 earthquake," Structures, vol. 40, pp. 386–402, Jun. 2022, doi: 10.1016/j.istruc.2022.04.026.

[7] F. Graziotti, U. Tomassetti, S. Sharma, L. Grottoli, and G. Magenes, "Experimental response of URM single leaf and cavity walls in out-of-plane two-way bending generated by seismic excitation," Constr. Build. Mater., vol. 195, pp. 650–670, Jan. 2019, doi: 10.1016/j.conbuildmat.2018.10.076.

[8] E. Işık et al., "Structural damages in masonry buildings in Adıyaman during the Kahramanmaraş (Turkiye) earthquakes (Mw 7.7 and Mw 7.6) on 06 February 2023," Eng. Fail. Anal., vol. 151, p. 107405, Sep. 2023, doi: 10.1016/j.engfailanal.2023.107405.

[9] L. Sorrentino, R. Masiani, and M. C. Griffith, "The vertical spanning strip wall as a coupled rocking rigid body assembly," Struct. Eng. Mech., vol. 29, no. 4, pp. 433–453, Jul. 2008, doi: 10.12989/SEM.2008.29.4.433.

DOI: https://doi.org/10.5592/CO/3CroCEE.2025.28

[10] L. F. Restrepo Vélez, G. Magenes, and M. C. Griffith, "Dry Stone Masonry Walls in Bending—Part I: Static Tests," Int. J. Archit. Herit., vol. 8, no. 1, pp. 1–28, Jan. 2014, doi: 10.1080/15583058.2012.663059.
[11] D. D'Ayala and Y. Shi, "Modeling Masonry Historic Buildings by Multi-Body Dynamics," Int. J. Archit. Herit., vol. 5, no. 4–5, pp. 483–512, Jul. 2011, doi: 10.1080/15583058.2011.557138.
[12] S. Lagomarsino, "Seismic assessment of rocking masonry structures," Bull. Earthq. Eng., vol. 13, no. 1, pp. 97–128, Jan. 2015, doi: 10.1007/s10518-014-9609-x.
[13] U. Tomassetti, A. A. Correia, P. X. Candeias, F. Graziotti, and A. Campos Costa, "Two-way bending out-of-plane collapse of a full-scale URM building tested on a shake table," Bull. Earthq. Eng., vol. 17, no. 4, pp. 2165–2198, Apr. 2019, doi: 10.1007/s10518-018-0507-5.
[14] M. Mongelli, A. Giocoli, I. Roselli, G. D. Canio, G. D. Felice, and S. D. Santis, "SHAKING TABLE TESTS ON C-SHAPED MASONRY WALLS: DISPLACEMENT FIELD DATA DETECTED BY 3D MOTION CAPTURE SYSTEM AT ENEA CASACCIA RESEARCH CENTER".
[15] F. Graziotti, U. Tomassetti, S. Kallioras, A. Penna, and G. Magenes, "Shaking table test on a full scale URM cavity wall building," Bull. Earthq. Eng., vol. 15, no. 12, pp. 5329–5364, Dec. 2017, doi: 10.1007/s10518-017-0185-8.
[16] S. Kallioras, A. A. Correia, P. X. Candeias, A. Campos Costa, and F. Graziotti, "Dataset from the dynamic shake-table experiments on a full-scale unreinforced clay-brick masonry building with chimneys," Data Brief, vol. 52, p. 109813, Feb. 2024, doi: 10.1016/j.dib.2023.109813.
[17] D. S. Panella, M. E. Tornello, and C. D. Frau, "A simple and intuitive procedure to identify pulse-like ground motions," Soil Dyn. Earthq. Eng., vol. 94, pp. 234–243, Mar. 2017, doi: 10.1016/j.soildyn.2017.01.020.